Solomon, I. (1955) *Phys. Rev. 99*, 559–565.
Switzer, R. L. (1971) *J. Biol. Chem. 246*, 2447–2458.
Tebar, A. R., Ballesteros, A., & Soria, J. (1977) *Experientia 33*, 1292–1293.
Umezu, K., Amaya, T., Yashimoto, A., & Tomita, K. (1971) *J. Biochem. (Tokyo) 70*, 249–262.
Victor, J., Greenberg, L. B., & Sloan, D. L. (1979) *J. Biol. Chem. 254*, 2647–2655.

Role of Metal Cofactors in Enzyme Regulation. Differences in the Regulatory Properties of the *Escherichia coli* Nicotinamide Adenine Dinucleotide Specific Malic Enzyme Depending on Whether Mg^{2+} or Mn^{2+} Serves as Divalent Cation†

Judi A. Milne and Robert A. Cook*

ABSTRACT: A number of differences in the kinetic properties of the *Escherichia coli* nicotinamide adenine dinucleotide (NAD^+) dependent malic enzyme have been found depending upon whether Mg^{2+} or Mn^{2+} served to fulfill the divalent cation requirement. With Mg^{2+} as cation, the velocity–malate saturation curve in the absence of effectors is complex at pH 7.4, indicating a combination of apparent positive and negative cooperativity, while the velocity-free Mg^{2+} saturation curve exhibits positive cooperativity. If Mn^{2+} served as cation, however, the velocity–malate and velocity-free Mn^{2+} saturation curves exhibit a simple hyperbolic response. The velocity–NAD^+ saturation curves, in contrast, exhibit a simple hyperbolic response in the presence of either metal cofactor, but the affinity for NAD^+ and the V_{max} are increased in the presence of Mn^{2+}. When Mg^{2+} serves as cation, the enzyme activity is much more sensitive to regulation by the allosteric inhibitor CoA and the allosteric activator aspartate. If Mn^{2+} replaces Mg^{2+}, the enzyme activity is more sensitive to inhibition by ATP. This inhibition is shown to be due to chelation but may be of physiological importance. The inhibitor, CoA, increases the interaction between malate-binding sites in the presence of Mn^{2+} but has little effect on subunit interaction in the presence of Mg^{2+}. The kinetic data can be explained by a model involving sequential ligand-induced conformational changes of the enzyme, resulting in a mixture of apparent positive and negative cooperative behavior. Alternate explanations involving different classes of noninteracting binding sites or different enzyme forms are also considered. The metal cofactors Mg^{2+} and Mn^{2+} appear to stabilize two distinct forms of the enzyme which differ in response to varying substrate and effector concentrations. The results are strikingly similar to previous results reported on the NAD^+-dependent isocitrate dehydrogenase, supporting the suggestion that metal cofactors function as regulatory entities.

The NAD^+-specific[1] malic enzyme (EC 1.1.1.38) of *Escherichia coli* has been reported to exhibit characteristics of a modulator dependent cooperative (MDC) system (Sanwal, 1970a); i.e., the substrates, malate and NAD^+, exhibit normal hyperbolic behavior in the absence of effectors, but cooperative behavior in the presence of allosteric inhibitors (Sanwal, 1970b; Yamaguchi et al., 1974). The enzyme has been shown to be specifically inhibited by CoA, acetyl-CoA, and ATP and activated by aspartate (Takeo et al., 1967; Sanwal, 1970b; Yamaguchi et al., 1974). The catalytic and regulatory properties of the enzyme have been determined almost exclusively in the presence of Mn^{2+} as the required cofactor, although the divalent cation requirement can be fulfilled by Mg^{2+} (Takeo et al., 1967; Takeo, 1969; Sanwal, 1970b; Murai et al., 1972; Yamaguchi et al., 1974). In view of the recent results reported with the NAD^+-specific isocitrate dehydrogenase suggesting that the metal cofactors, Mg^{2+} and Mn^{2+}, may possibly function as allosteric effectors (Barratt & Cook, 1978), a detailed examination of the function of metal cofactors in the NAD^+-specific malic enzyme system as well as other enzyme systems capable of utilizing Mg^{2+} and Mn^{2+} is warranted. Distinct effects of Mg^{2+} and Mn^{2+} on the NAD^+-specific malic enzyme have, in fact, been reported by Yamaguchi et al. (1974), primarily in regard to aspartate activation. In their study, it was reported that (1) the enzyme was more sensitive to inhibition by CoA in the presence of Mg^{2+}; (2) the interaction between malate-binding sites was weakly cooperative in the presence of Mg^{2+}; (3) high concentrations of aspartate were inhibitory only in the presence of Mn^{2+}; and (4) Mg^{2+} and Mn^{2+} exhibited sigmoidal behavior in the absence of effectors. A definitive role for the metal cofactor in the enzyme mechanism was not suggested, however, from these preliminary results.

Since the substrates and effectors utilized in the present study are capable of chelating Mg^{2+} and Mn^{2+} to different extents, the experimental data was routinely subjected to computer analysis to determine the concentration of the various free and chelated forms of all ligands. Such analyses have allowed us to distinguish true allosteric effects from simple

† From the Department of Biochemistry, University of Western Ontario, London, Ontario, Canada. *Received August 16, 1978; revised manuscript received November 30, 1978.* This work was supported by Grant No. MA-3848 from the Medical Research Council of Canada.

[1] Abbreviations used: NAD^+, nicotinamide adenine dinucleotide; NADH, reduced NAD^+; $NADP^+$, NAD^+ phosphate; CoA, coenzyme A; n_H, Hill coefficient or interaction coefficient; V_{max}, maximum velocity; $S_{0.5}$, half-saturating concentration of substrate; $I_{0.5}$, concentration of inhibitor giving 50% inhibition; $NaDodSO_4$, sodium dodecyl sulfate; Tris, 2-amino-2-hydroxymethyl-1,3-propanediol; EDTA, (ethylenedinitrilo)-tetraacetic acid.

0006-2960/79/0418-3604$01.00/0

chelating effects. The results from such analysis reveal a more complex kinetic response in the presence of Mg^{2+} than previously reported, involving a mixture of apparent positive and negative cooperative behavior. As a result of this complexity, the previously proposed mechanism for the enzyme (Sanwal, 1970b) in terms of the two-state model of Monod et al. (1965) must be extensively modified or, alternatively, discarded. The results are strikingly similar to the results previously obtained with isocitrate dehydrogenase (Barratt & Cook, 1978), supporting the suggestion that metal cofactors may function as allosteric effectors. Similar studies on the role of Mg^{2+} and Mn^{2+} on the NADP-specific malic enzyme of *E. coli* will be reported in a subsequent paper.

Experimental Section

Materials. The NAD^+-specific malic enzyme used here was purified from both *E. coli* strain K12 (HfrH) and a mutant of this strain which lacked malate dehydrogenase activity, kindly provided by Dr. B. D. Sanwal. The use of the mutant strain was advantageous as NAD^+-specific malate dehydrogenase activity interferes with the assay of NAD^+-specific malic enzyme activity. The parent and mutant strains of *E. coli* were grown on LB media composed of 1% bactotryptone, 0.5% yeast extract, and 1% NaCl, pH 7.0. Large scale growths of the organism (800L) were carried out at Labatts Brewery Co., London, Ontario. Following a 1% inoculum, the cells were grown to the late logarithmic phase (approximately 6 h), resulting in 4.5 g of cells/L of media. The cells were wet packed by centrifugation and stored at −20 °C.

The enzyme was purified essentially as described by Yamaguchi et al. (1973) with the modification that the cells were disrupted in the French pressure cell. The cells were thus disrupted and subjected to streptomycin treatment, ammonium sulfate fractionation, heat and acid treatment, calcium phosphate gel adsorption, DEAE-Sephadex A-50 column chromatography, hydroxylapatite column chromatography, and finally Sepharose 6B column chromatography as described by Yamaguchi et al. (1973). The final enzyme preparation was stored in a minimal volume of 100 mM Tris-HCl, pH 7.4, containing 10 mM $MgCl_2$, 5 mM 2-mercaptoethanol, and 5 mM L-aspartate at 4 °C. The enzyme was stable for 3–4 months under these conditions. Homogeneous enzyme was not always obtained following this procedure. In the experimental results presented here, enzyme preparations with specific activities from 45 to 238 were used (1 unit is defined as the formation of 1 μmol of NADH min^{-1} (mg of protein)$^{-1}$). The homogeneity of the enzyme preparations was routinely tested by polyacrylamide gel electrophoresis following the method of Davis (1964). Enzyme preparations with specific activity of 238 were homogeneous, but preparations with specific activities of 45, 73, and 120 exhibited one major band and varying concentrations of minor bands when the gels were stained with Coomassie blue or Amido black 10B (50–100 μg of protein applied). A single band, corresponding to the major protein band, was observed when the gels were stained specifically for NAD^+-specific malic enzyme activity. All enzyme preparations were free of the following enzymes tested, which could interfere with the kinetic assay: malate dehydrogenase, malate oxidase, $NADP^+$-specific malic enzyme, and NADH oxidase. The results obtained with all enzyme preparations were identical, indicating that the unusual kinetic effects observed were not due to the trivial explanation of contaminating enzyme activities.

The molecular weight of the homogeneous enzyme was estimated at 268 000 by the method of polyacrylamide gel electrophoresis (Zwaan, 1967; Matagne & Schlosser, 1977). $NaDodSO_4$ gel electrophoresis following the procedure of Weber & Osborn (1969) revealed a single band with an estimated molecular weight of 63 000. The enzyme is therefore composed of four subunits of identical molecular weight in agreement with the results of Yamaguchi et al. (1973).

NAD^+, L-malate, L-aspartate, ATP, and coenzyme A were purchased from Sigma Chemical Co. and Boehringer-Mannheim Co. The $MnCl_2$ and $MgCl_2$ were analytical grade and purchased from J. T. Baker Chemical Co.

Kinetic Measurements. Solutions of NAD^+, $MnCl_2$, ATP, and coenzyme A were prepared just before use. All kinetic measurements were performed at 25–26 °C with a Gilford recording spectrophotometer, Model 2400, equipped with dual thermoplates and a Haake thermostat. The enzyme to be used was diluted and dialyzed for 24 h against three changes of 50 mM Tris-HCl buffer, pH 7.4, containing 0.1 mM NaEDTA and 0.5 mM 2-mercaptoethanol at 4 °C. Extensive dialysis was required to remove the $MgCl_2$ and aspartate used to stabilize the enzyme during storage. To ensure that no denaturation occurred during the course of the experiment, the enzyme was checked periodically by using the standard assay mixture, containing 50 mM Tris-HCl, pH 7.4, 2.0 mM NAD^+, 2.5 mM L-malate, and 5.0 mM $MgCl^2$ in a total volume of 1.0 mL. The reaction velocity was measured by monitoring the production of NADH at 340 nm in a quartz cuvette of 1-cm light path and 1.4-mL volume. Addition of all reactants to the cuvette were made by μL pipets and/or Hamilton syringes as warranted.

The kinetic behavior of the enzyme was studied in detail, i.e., 20–40 experimental points were routinely attempted per individual curve with duplicate and overlapping points in concentration ranges necessitating dilutions. Temperature equilibration was attained by allowing the cuvettes to stand in the thermostated cuvette holder for 10 min. The reaction was routinely initiated by the addition of L-malate. Control experiments revealed essentially identical results when the reaction was initiated with enzyme, metal cofactor or NAD^+.

Metal Chelation Analysis. All the data obtained in the present study have been routinely subjected to computer analysis by utilizing a slightly modified version of the program developed by Perrin & Sayce (1967) to determine the free metal ion concentration and the various free and metal-chelated forms of all ionic species of ligand present. In addition, the binding of metals to the buffer species, free base 2-amino-2-hydroxymethyl-1,3-propanediol, chloride ion, and EDTA (5 μM in all assays) was also considered. However, at the concentrations of these species which were present, the inclusion of these complexes in the calculations influences the concentrations of free metal and all ionic forms of ligand by less than 1%. Therefore, the formation of these complexes is routinely neglected in the calculations here presented.

The following literature values (O'Sullivan, 1969; O'Sullivan & Perrin, 1964; Coleman, 1972; Apps, 1973) for the log stability constants have been used in this study: $Mg–ATP^{2-}$, 4.30; $Mn–ATP^{2-}$, 4.88; Mg–malate, 1.6; Mn–malate, 2.2; Mg–NAD, 1.71; Mn–NAD, 1.89; Mn–aspartate, 3.7 Mg–aspartate, 2.4; Mn–CoA, 2.4; Mg–CoA, 2.0.

Results

The results of previous kinetic studies with NAD^+-specific malic enzyme of *E. coli* were obtained at pH 7.0 (Sanwal, 1970b) or at pH 7.9 (Yamaguchi et al., 1974). All kinetic studies reported here have been performed in 0.05 M Tris-HCl buffer, pH 7.4, the optimum pH for enzyme activity. The pH of all stock substrate and effector solutions was therefore

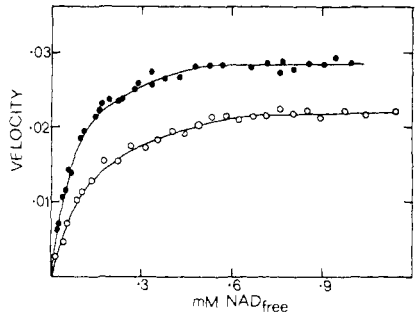

FIGURE 1: Initial velocity kinetic studies with varying NAD^+ concentration and a fixed, saturating concentration of malate (2.5 mM) and divalent cation. The data are presented in terms of the calculated free NAD^+ concentration. The resultant kinetic constants for both free and total NAD^+ concentration are summarized in Table I. Conditions: 50 mM Tris-HCl buffer, pH 7.4, 25 °C. Velocity is expressed as μmol of NADH formed/min. (○) Presence of saturating Mg^{2+} (5.0 mM); (●) presence of saturating Mn^{2+} (0.3 mM).

Table I: Kinetic Constants for Malic Enzyme[a]

variable substrate	cation	$S_{0.5}$ (mM)	n_H[b]
Mg^{2+} (total)		0.80	1.7/2.4[c]
Mg^{2+} (free)		0.67	1.8
NAD^+ (total)	Mg^{2+}	0.175	1.03
NAD^+ (free)	Mg^{2+}	0.100	1.03
malate (total)	Mg^{2+}	0.35[d]	1.4/3.8
malate (free)	Mg^{2+}	0.32[d]	1.4/3.8
Mg^{2+}-malate		0.06[d]	1.4/3.8
Mg^{2+}-NAD		0.030	1.03
Mn^{2+} (total)		0.022	1.05
Mn^{2+} (free)		0.019	1.02
NAD^+ (total)	Mn^{2+}	0.073	1.02
NAD^+ (free)	Mn^{2+}	0.072	1.02
malate (total)	Mn^{2+}	0.147	1.04
malate (free)	Mn^{2+}	0.141	1.03
Mn^{2+}-malate		0.006	1.02
Mn^{2+}-NAD		0.002	1.02

[a] Kinetic constants for the variable substrate have been determined at saturating concentrations of all other fixed ligands. [b] Interaction coefficients determined from the slopes of the Hill plots. [c] The biphasic nature of this curve disappeared when corrected for chelation. [d] The $S_{0.5}$ values are not equivalent to the K_m values in view of the biphasic nature of the saturation curves, but are included here for comparative purposes.

adjusted to pH 7.4 to ensure that the pH was maintained in all enzyme assays.

Initial Velocity Studies in the Absence of Allosteric Effectors. When the velocity of the reaction is studied as a function of NAD^+ concentration in the presence of saturating concentrations of malate (2.5 mM) and either Mn^{2+} (0.3 mM) or Mg^{2+} (5.0 mM) at pH 7.4, a hyperbolic response is obtained (Figure 1). Double-reciprocal plots of the data are typically linear (see Figure 7). The data have been presented in terms of the free NAD^+ concentration. The V_{max} is increased approximately 40% in the presence of Mn^{2+} as estimated from double-reciprocal plots of the data. Hill plots of the data indicated n_H values of 1.0 for NAD^+ in the presence of either metal cofactor. The kinetic constants for both free and total NAD^+ concentrations are summarized in Table I.

When the velocity of the reaction is studied as a function of the free malate concentration at saturating NAD^+ (1–2 mM) at pH 7.4, the saturation curves obtained in the presence of Mg^{2+} and Mn^{2+} are strikingly different (Figure 2A). In the presence of Mg^{2+} (5.0 mM), a complex sigmoidal saturation curve is obtained containing an intermediary plateau region, while in the presence of Mn^{2+} (0.3 mM) an apparent hyperbolic response is observed. Double-reciprocal plots of

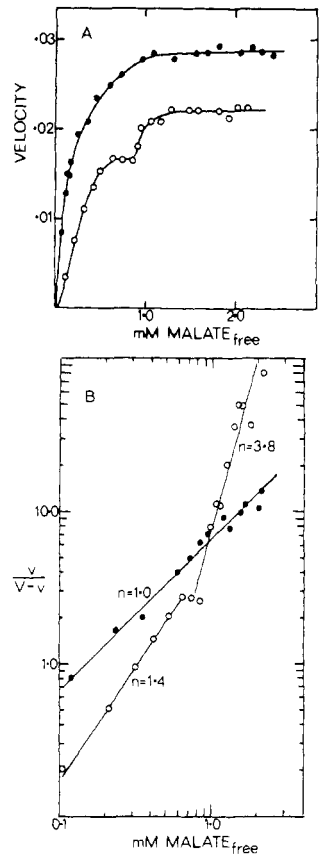

FIGURE 2: Initial velocity kinetic studies with varying malate concentration and a fixed, saturating concentration of NAD^+ and divalent cation. The data are presented in terms of the calculated free malate concentration. The resultant kinetic constants for both free and total malate concentration are summarized in Table I. Conditions: 50 mM Tris-HCl buffer, pH 7.4, 25 °C. Velocity is expressed as μmol of NADH formed/min. (○) Presence of saturating Mg^{2+} (5.0 mM) and NAD^+ (2.0 mM); (●) presence of saturating Mn^{2+} (0.3 mM) and NAD^+ (1.0 mM). (A) Saturation curves; (B) Hill plots. The V_{max} values required for the Hill plots have been estimated from the double-reciprocal plots. The V_{max} values used are 0.0227 and 0.0317 in the presence of Mg^{2+} and Mn^{2+}, respectively.

the data are typically linear in the presence of Mn^{2+} but are complex in the presence of Mg^{2+}. The values for V_{max} have been estimated from the intercepts of the double-reciprocal plots to be 0.0227 and 0.0317 in the presence of Mg^{2+} and Mn^{2+}, respectively. While the determination of V_{max} is a simple procedure from the linear plots, estimation of the V_{max} value from the complex plots is difficult. This problem is discussed in detail in the Discussion section. When the data are replotted in the form of the Hill plot by using the above V_{max} values (Figure 2B), the n_H value for malate in the presence of Mn^{2+} is 1.0, while, in the presence of Mg^{2+}, a biphasic curve is obtained with n_H values of 1.4 and 3.8. The resultant kinetic constants for free and total malate concentration are summarized in Table I.

When the velocity of the reaction is studied as a function of free cation concentration at saturating malate (2.5 mM) and NAD^+ (1.0 mM in the presence of Mn^{2+}, 2.0 mM in the presence of Mg^{2+}) at pH 7.4, the saturation curves for Mg^{2+} and Mn^{2+} are strikingly different (Figure 3). A sigmoidal saturation curve for free Mg^{2+} is observed, while a hyperbolic response is observed with free Mn^{2+}. When the data are presented in the Hill plot (not shown), n_H values of 1.8 and 1.0 are obtained for free Mg^{2+} and free Mn^{2+}, respectively. The resultant kinetic constants for total and free metal cofactor concentrations are summarized in Table I.

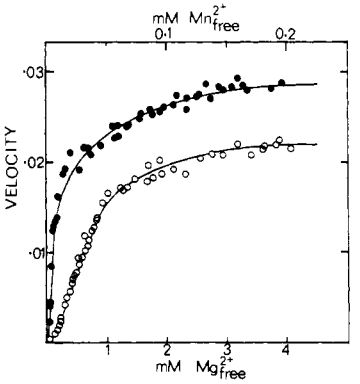

FIGURE 3: Initial velocity kinetic studies with varying divalent cation concentration and a fixed, saturating concentration of malate (2.5 mM) and NAD^+ (2.0 mM). The data are presented in terms of the calculated free cation concentration. The resultant kinetic constants for free and total cation concentrations are summarized in Table I. Conditions: 50 mM Tris-HCl buffer, pH 7.4, 25 °C. Velocity is expressed as μmol of NADH formed/min. (○) Varying Mg^{2+} concentration; (●) varying Mn^{2+} concentration.

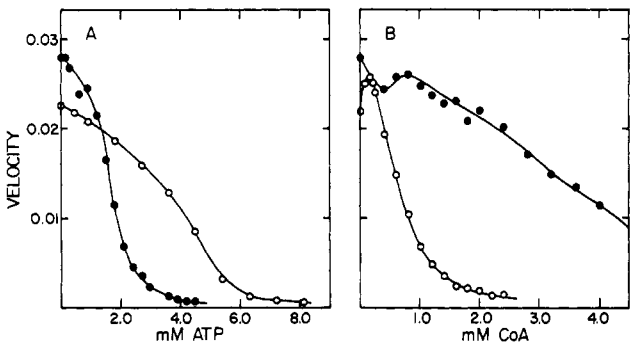

FIGURE 4: The effect of the inhibitors, ATP and CoA, on the velocity of the reaction in the presence of fixed, saturating concentrations of malate, NAD^+, and divalent cation. Conditions: 50 mM Tris-HCl buffer, pH 7.4, 25 °C. Velocity is expressed as μmol of NADH formed/min. (A) Inhibition studies with ATP. (●) In the presence of fixed, saturating concentrations of Mn^{2+} (1.0 mM), malate (2.5 mM), and NAD^+ (1.0 mM); (○) in the presence of fixed, saturating concentrations of Mg^{2+} (5.0 mM), malate (2.5 mM), and NAD^+ (2.0 mM). (B) Inhibition studies with CoA. (●) In the presence of fixed, saturating concentrations of Mn^{2+} (0.3 mM), malate (2.5 mM), and NAD^+ (1.0 mM); (○) in the presence of fixed, saturating concentrations of Mg^{2+} (5.0 mM), malate (2.5 mM), and NAD^+ (2.0 mM).

Initial Velocity Studies in the Presence of Effectors. In view of the differences in kinetic properties of the enzyme with Mg^{2+} and Mn^{2+}, it was of interest to examine the effect of the known inhibitors, CoA and ATP, and the activator, aspartate, on the activity of the enzyme in the presence of either metal cofactor.

The effect of the inhibitors, ATP and CoA, on the velocity of the reaction in the presence of saturating concentrations of malate, NAD^+, and metal cofactor is presented in Figure 4. It is obvious from Figure 4A that ATP is a more effective inhibitor in the presence of Mn^{2+} than in the presence of Mg^{2+}. The concentration of total ATP resulting in 50% inhibition ($I_{0.5}$) is estimated at 1.6 mM and 3.9 mM in the presence of Mn^{2+} and Mg^{2+}, respectively. Since ATP is known to be a potent chelator of Mn^{2+} and Mg^{2+}, the data in Figure 4A were analyzed in terms of the various chelated and ionic forms of the ligands. The results of such analysis indicate that, at the concentration of ATP causing 50% inhibition with Mn^{2+}, the *free* Mn^{2+} concentration has been reduced to 0.019 mM, approximately the K_m value (0.016 mM). Thus, the inhibition by ATP appears to be due to simple chelation of essential Mn^{2+} rather than direct binding to the enzyme and resultant allosteric effects. Similar results are obtained from an analysis of the data obtained in the presence of Mg^{2+}.

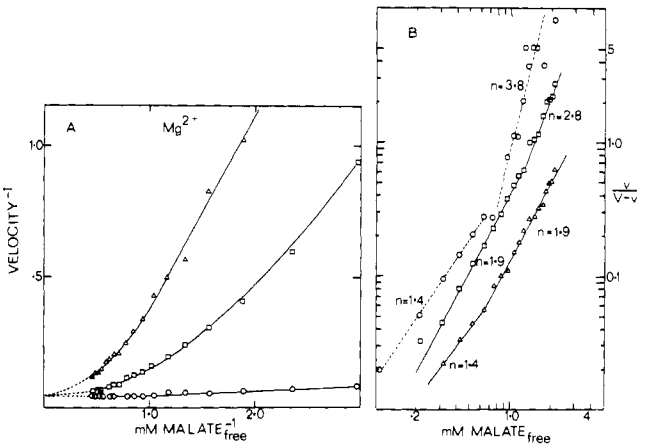

FIGURE 5: The effect of the inhibitor, CoA, on initial velocity kinetic studies with varying malate concentration and a fixed, saturating concentration of NAD^+ (2.0 mM) and Mg^{2+} (5.0 mM). The data are presented in terms of the calculated free malate concentration. Conditions: 50 mM Tris-HCl buffer, pH 7.4, 26 °C. Velocity is expressed as μmol of NADH formed/min. (○) In the absence of CoA; (□) in the presence of 0.4 mM CoA; (△) in the presence of 0.8 mM CoA. (A) Double-reciprocal plots. For a fine detail plot in the absence of CoA, see Figure 2B. (B) Hill plots. A value for V_{max} of 0.0227 from the uninhibited curve has been used for the calculation of all Hill plots (see text).

In contrast to the effects of ATP, CoA appears to be a more effective inhibitor in the presence of Mg^{2+} than in the presence of Mn^{2+} (Figure 4B). The interaction of CoA with the enzyme is complex, revealing slight activation (18%) at low CoA concentrations in the presence of Mg^{2+} and a small "trough" in the CoA inhibition curve in the presence of Mn^{2+}. The concentration of total CoA resulting in 50% inhibition is estimated at 0.75 mM and 3.4 mM in the presence of Mg^{2+} and Mn^{2+}, respectively. (In terms of free CoA concentration, 50% inhibition is estimated at 0.55 mM and 3.1 mM in the presence of Mg^{2+} and Mn^{2+}, respectively.) Experiments similar to those presented in Figure 4 have been performed at saturating concentrations of NAD^+ and metal cofactor, but at malate concentrations approximating the K_m value (0.5 mM in the presence of Mg^{2+}; 0.1 mM in the presence of Mn^{2+}). Under these conditions, similar inhibition curves are observed with ATP, but the activation observed at low CoA concentrations is not observed. The concentration of ATP resulting in 50% inhibition is reduced to 1.2 mM and 2.6 mM in the presence of Mn^{2+} and Mg^{2+}, respectively. The concentration of CoA resulting in 50% inhibition is also reduced to 0.12mM and 0.35mM in the presence of Mg^{2+} and Mn^{2+}, respectively.

The effect of the inhibitor, CoA, on the velocity–substrate curves was then examined at two concentrations of inhibitor causing approximately 30% and 70% inhibition. The effect of the inhibitor, CoA, on initial velocity kinetic studies with varying malate concentration and a fixed, saturating concentration of NAD^+ (2.0 mM) and Mg^{2+} (5.0 mM) is presented in Figure 5. The double-reciprocal plots obtained for malate in the presence of 0.4 mM and 0.8 mM CoA appear to be simple parabolas containing no intermediary plateau regions (Figure 5A). The uninhibited curve also appears to be a simple parabola, but is identical with Figure 2B when plotted on an expanded scale. All curves appear to intersect at the vertical axis, indicative of pseudo-competitive inhibition, although the extrapolation of curves is always hazardous. For the Hill plots of the data (Figure 5B), the maximum velocity of the uninhibited curve (0.0227) has been used for all cases.

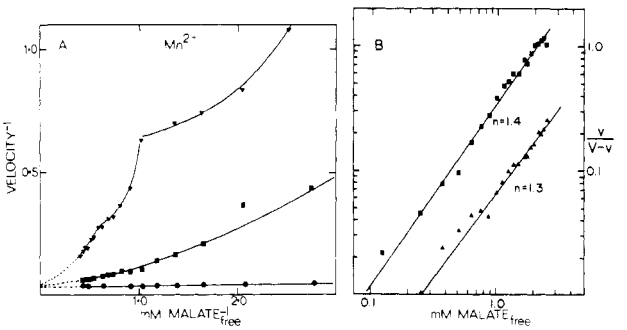

FIGURE 6: The effect of the inhibitor, CoA, on initial velocity kinetic studies with varying malate concentration and a fixed, saturating concentration of NAD^+ (1.0 mM) and Mn^{2+} (0.3 mM). The data are presented in terms of the calculated free malate concentration. Conditions: 50 mM Tris-HCl buffer, pH 7.4, 25 °C. Velocity is expressed as μmol of NADH formed/min. (●) In the absence of CoA; (■) in the presence of 2.0 mM CoA; (▲) in the presence of 4.0 mM CoA. (A) Double-reciprocal plots; (B) Hill plots. A value for V_{max} of 0.0317 has been used for the calculation of the inhibited and uninhibited curves.

The possible errors due to this assumption are discussed later. The Hill plots of the data are biphasic in all cases with n_H values for malate of 1.9 and 2.8 in the presence of 0.4 mM CoA, and 1.4 and 1.9 in the presence of 0.8 mM CoA. Although the n_H values vary slightly from the values obtained in the absence of CoA, it would appear that CoA, although a potent inhibitor of the velocity of the reaction, has little effect on the interaction between malate-binding sites in the presence of Mg^{2+}.

The effect of the inhibitor, CoA, on the initial velocity kinetic studies with varying malate concentration and a fixed, saturating concentration of NAD^+ (1.0 mM) and Mn^{2+} (0.3 mM) is presented in Figure 6. The double-reciprocal plots for malate, linear in the absence of CoA, reveal greater complexity in the presence of increasing concentrations of CoA. A simple parabola is observed at 2.0 mM CoA, but a more complex interaction at 4.0 mM CoA indicating a possible triphasic curve. As in the presence of Mg^{2+}, the curves appear to intersect near the vertical axis. Hill plots of data (Figure 6B), using a V_{max} of 0.0317 in all cases, indicate n_H values of 1.4 and 1.3 for the inhibited curve. A more complex Hill plot could have been presented for the data in the presence of 4.0 mM CoA, but a linear line appears to be consistent with the data, especially considering the error in measuring low velocities.

The effect of the inhibitor, CoA, on initial velocity kinetic studies with varying NAD^+ concentrations and a fixed, saturating concentration of malate (2.5 mM) and divalent cation is presented in Figure 7. The double-reciprocal plots of the data are linear in all cases and indicate noncompetitive inhibition by CoA in the presence of Mg^{2+} and Mn^{2+}. All lines have been determined by linear regression analysis. Other than inhibition, CoA appears to have no effect on the interaction between NAD^+ binding sites in the presence of Mg^{2+} (Figure 7A) or in the presence of Mn^{2+} (Figure 7B). Hill plots of the data indicate n_H values of 1.0 in all cases.

The effect of the activator, aspartate, on initial velocity kinetic studies with varying malate concentration and a fixed, saturating concentration of NAD^+ was then tested in the presence of saturating concentrations of Mg^{2+} and Mn^{2+}. It would appear from the data of Figure 8 that aspartate (at 2.0 mM) activates the enzyme in the presence of Mg^{2+} (Figure 8B), but not in the presence of Mn^{2+} (Figure 8A). In the presence of Mg^{2+}, aspartate abolishes the intermediary plateau region and the sigmoidal nature of the free malate saturation

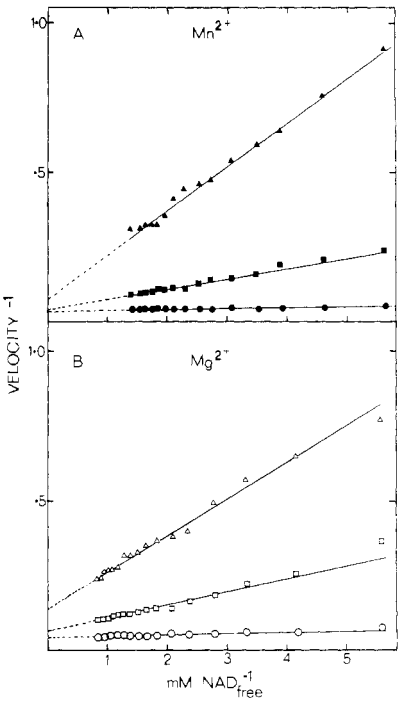

FIGURE 7: The effect of the inhibitor, CoA, on initial velocity kinetic studies with varying NAD^+ concentration and a fixed, saturating concentration of malate (2.5 mM) and divalent cation, presented in the double-reciprocal form. The data are presented in terms of the calculated free NAD^+ concentration. All lines are determined by linear regression analysis. Conditions: 50 mM Tris-HCl buffer, pH 7.4, 25 °C. Velocity is expressed as μmol of NADH formed/min. (A) In the presence of saturating Mn^{2+} (0.3 mM); (●) in the absence of CoA; (■) in the presence of 2.0 mM CoA; (▲) in the presence of 4.0 mM CoA. (B) In the presence of saturating Mg^{2+} (5.0 mM); (○) in the absence of CoA; (□) in the presence of 0.4 mM CoA; (△) in the presence of 0.8 mM CoA.

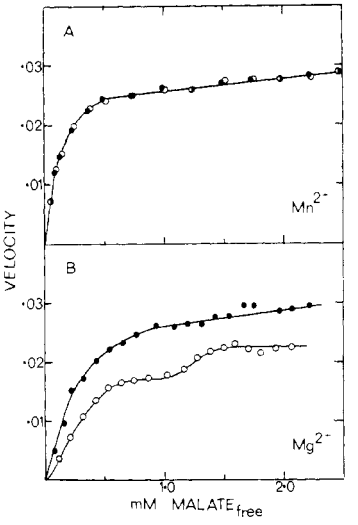

FIGURE 8: The effect of the activator, aspartate (2.0 mM), on initial velocity kinetic studies with varying malate concentration and a fixed, saturating concentration of NAD^+ and divalent cation. The data are presented in terms of the calculated free malate concentration. Conditions: 50 mM Tris-HCl buffer, pH 7.4, 25 °C. Velocity is expressed as μmol of NADH formed/min. (A) In the presence of saturating Mn^{2+} (0.3 mM) and NAD^+ (1.0 mM); (●) in the absence of aspartate; (○) in the presence of 2.0 mM aspartate; (◑) overlapping points. (B) In the presence of saturating Mg^{2+} (5.0 mM) and NAD^+ (2.0 mM); (○) in the absence of aspartate; (●) in the presence of 2.0 mM aspartate.

curve. Hill plots of the data (not shown) in the presence of Mg^{2+} are biphasic in the absence of aspartate with n_H values of 1.6 and 6.0, but indicate an n_H value of 1.0 in the presence

of aspartate. Hill plots for malate in the presence of Mn^{2+} reveal an n_H value of 1.0 in the presence or absence of aspartate.

Discussion

We have chosen, in this study, to present the data in the form of the Hill plot due to the usefulness of this representation in the interpretation of complex subunit interaction (Cook & Koshland, 1970; Cornish-Bowden & Koshland, 1975). By this procedure curved Hill plots have been observed in enzyme systems exhibiting no obvious intermediary plateau regions, demonstrating that the overall shape of the curve is the important criteria (Cook & Koshland, 1970). This representation of the data does, however, require a reasonably accurate value for V_{max} which is often difficult to obtain from enzyme systems exhibiting positive or negative cooperativity. In the present study, little difficulty is encountered in determining V_{max} in the presence of Mn^{2+}, where the data are normally Michaelis–Menten. However, in the presence of Mg^{2+}, the curves in most cases exhibit a combination of apparent positive and negative cooperative behavior making the values for V_{max} somewhat ambiguous. We have analyzed all of our data using several V_{max} values to determine whether the biphasic nature of the curves could be abolished. Under no circumstances did this occur, although the absolute n_H values, especially above 50% saturation, are sensitive to the V_{max} values (compare n_H values from Figures 2 and 8). Lower V_{max} values raise the n_H values, while higher V_{max} values decrease this value. On examination of the data of Figure 6, for example, if a value for V_{max} is chosen which is 50% lower than the 0.0317 value of the uninhibited curve, the n_H value is increased from 1.3 to 1.6 and the apparent plateau regions (not drawn in) appear more exaggerated. Thus, the n_H values presented in this study represent (in most cases) the minimum value for n_H. Since the absolute n_H values are not critical to the interpretation of the data, we are confident that any errors in the determination of V_{max} do not negate the results presented in this study.

The recent studies on the role of metal cofactors in enzyme regulation from this laboratory have revealed a number of significant differences in the catalytic and regulatory properties of the NAD^+-specific isocitrate dehydrogenase depending upon whether Mg^{2+} or Mn^{2+} served to fulfill the divalent metal cation requirement (Barratt & Cook, 1978). The results obtained with the NAD^+-specific malic enzyme reported here are strikingly similar to the results obtained with the isocitrate dehydrogenase system. The metal cofactors, Mn^{2+} and Mg^{2+}, appear to stabilize two distinct forms of the NAD^+-specific malic enzyme, presumably by inducing different changes in conformation or structure of the enzyme. In the "Mn^{2+}–enzyme", no cooperativity between malate-binding sites or Mn^{2+}-binding sites is observed in the absence of allosteric effectors (Figures 2 and 3), indicating that the binding sites for malate (and Mn^{2+}) are most likely equivalent and independent. In the "Mg^{2+}–enzyme", however, positive cooperativity between Mg^{2+}-binding sites is observed (Figure 3) and complex interaction between malate-binding sites (Figure 2). The observed results can be explained on the basis of a model involving ligand-induced sequential changes in enzyme conformation (Koshland et al., 1966). The complex Hill plots presented in Figures 2B and 5B can be interpreted as original positive cooperativity between malate-binding sites, followed by negative cooperativity and finally positive cooperativity (Cornish-Bowden & Koshland, 19755). An explanation of the complex malate saturation curves in terms of a model involving preexisting dissimilar sites appears unlikely in view of the results obtained with the Mn^{2+}–enzyme. The absence of cooperativity between NAD^+-binding sites indicates that the binding sites for NAD^+ are most likely equivalent and independent in both the Mn^{2+}– and Mg^{2+}–enzyme (Figure 1).

The hypothesis that Mg^{2+} and Mn^{2+} stabilize two distinct forms of enzyme is supported by the varied response of the two enzyme forms to inhibitors and activators presented in Figures 4–8. Thus, the Mg^{2+}–enzyme appears to be more sensitive to inhibition by CoA and activation by aspartate, while the Mn^{2+}–enzyme is more sensitive to inhibition by ATP. The inhibition by CoA appears to be allosteric in nature in agreement with the results of previous studies (Sanwal, 1970b; Yamaguchi et al., 1974). In the case of the Mg^{2+}–enzyme, the assumed conformational change caused by CoA binding causes inhibition but does not effect the interaction between malate-binding sites or NAD^+-binding sites (see Figures 5 and 7). In the case of the Mn^{2+}–enzyme, the conformational change induced by CoA does increase the interaction between malate-binding sites (Figure 6) but does not affect the interaction between NAD^+-binding sites (Figure 7). These observations substantiate the hypothesis that the structure of the enzyme differs in the presence of Mg^{2+} and Mn^{2+}.

In contrast to the results obtained with CoA, the Mg^{2+}–enzyme is less sensitive to inhibition by ATP than the Mn^{2+}–enzyme. Analysis of the results in terms of the various free and chelated forms of substrate has indicated that inhibition by ATP is due to chelation rather than specific allosteric effects, confirming the suggestion of Yamaguchi et al. (1974). Despite the fact that this inhibition is of a nonspecific nature, the potent inhibition by ATP, especially at a nonsaturating concentration of malate, should be considered of physiological importance (Rose, 1968). From the data presented in Figure 8, it would appear that the allosteric site for the activator, aspartate, is functional only in the Mg^{2+}–enzyme. The observed activation by aspartate can be explained by assuming that aspartate binds to an allosteric site of the Mg^{2+}–enzyme resulting in a conformational change which increases the affinity of the enzyme for malate and abolishes the mixed cooperativity between malate-binding sites. The explanation for the lack of any effect by aspartate in the Mn^{2+}–enzyme is complicated by the observation that the free Mn^{2+} concentration has been reduced to a level causing an expected 25–30% inhibition of the velocity. Since no inhibition is observed, we would conclude that the enzyme is activated by aspartate to the same extent as in the presence of Mg^{2+}, but this activation is balanced by the inhibition due to Mn^{2+} chelation. When Mg^{2+} was used as the metal cofactor, the free Mg^{2+} level was not significantly altered by the presence of aspartate.

There are some significant differences between the results reported here and those reported previously by Yamaguchi et al. (1974). The previously unobserved complex interaction between malate-binding sites in the Mg^{2+}–enzyme reported here can be explained simply by the finer detail of the present study. The second discrepancy is the absence of any cooperativity between Mn^{2+}-binding sites (Figure 3) and the lack of activation by aspartate in the Mn^{2+}–enzyme (Figure 8) noted in this study. Two possible explanations of these anomalies are (i) the Mg^{2+} used to stabilize the enzyme during storage was not completely removed in prior studies (Yamaguchi et al., 1973, 1974) or (ii) previous kinetic data obtained with the enzyme have not been subjected to analysis in terms of the *free* Me^{2+} concentration.

The results of previous studies with the NAD^+-specific malic enzyme performed in the presence of Mn^{2+} have been interpreted in terms of a two-state model of Monod et al. (1965).

The results obtained in the present study with Mn^{2+} as the required cofactor are consistent with this interpretation. However, the complex interactions observed between substrate-binding sites in the presence of Mg^{2+} cannot be accommodated by the simple two-state model. We have suggested a model for the enzyme involving sequential ligand-induced changes in enzyme conformation (Koshland et al., 1966) resulting in mixed positive and negative cooperative behavior. A similar explanation has been suggested for the binding of Mn^{2+} and malate to the NADP-specific malic enzyme of pigeon liver (Hsu & Lardy, 1967; Hsu et al., 1976). Similar observed intermediary plateau regions have been explained on the basis of extreme negative cooperativity resulting in "half-site reactivity" (Hsu et al., 1976). As in the pigeon liver case, an alternate explanation involving two classes of structurally dissimilar Mn^{2+} or malate binding sites in the enzyme cannot be excluded in the present study. The enzyme has been shown to be composed of four subunits of identical molecular weight in the present study and by Yamaguchi et al. (1973). While the complete identity of the subunits has not been established, an explanation involving nonidentical subunits is not likely in view of the results obtained with the Mn^{2+}–enzyme, indicating that the substrate sites are equivalent in the native enzyme.

In the present study, we have suggested that Mg^{2+} and Mn^{2+} may stabilize two distinct conformational forms of the *same* enzyme which differ in response to varying substrate and effector concentrations. An interesting alternative is the possibility of two distinct NAD^+-specific malic enzymes, one displaying hyperbolic kinetics with a high affinity for substrates (the Mn^{2+}–enzyme) and a second displaying sigmoidal kinetics with a low affinity for substrates (the Mg^{2+}–enzyme). In this model, the two enzyme forms could not be in equilibrium to be consistent with the observed results.

Thus the complex velocity–malate curves in the presence of Mg^{2+} (Figures 2 and 8) could be explained by assuming malate could react with both forms of enzyme, albeit with different affinity. This explanation implies that both the Mn^{2+}–enzyme and Mg^{2+}–enzyme are capable of utilizing Mg^{2+} and it is surprising that a more complex Mg^{2+} saturation curve is not observed. Although only one active form of enzyme is observed in disc gel electrophoresis with either Mg^{2+} or Mn^{2+}, this evidence is not sufficient to rule out such a two-state model. Preliminary results from this laboratory indicate that Mg^{2+} and Mn^{2+} do not alter the molecular weight of the enzyme (R. A. Cook, unpublished results), indicating that the Mg^{2+}– and Mn^{2+}–enzymes forms do not occur via a ligand-induced association–dissociation mechanism.

Several enzymes have been shown to have different regulatory properties in the presence of Mg^{2+} and Mn^{2+}, including ADP-glucose pyrophosphorylase (Gentner & Preiss, 1968), glutamine synthetase (Deuel & Stadtman, 1970; Segal & Stadtman, 1972a,b), pyruvate kinase (Gabrielle & Baldi, 1973), and several gluconeogenic enzymes (Wimhurst & Manchester, 1970). It is obvious from the results presented in this study that the catalytic and regulatory properties of the NAD^+-specific malic enzyme are also significantly altered by the choice of metal cofactor. Our results indicate that the Mg^{2+}–enzyme exhibits complex subunit interactions and is much more sensitive to regulation by CoA and aspartate. If Mn^{2+} replaces Mg^{2+} as the required cofactor, the enzyme has a greater affinity for substrates, exhibits no subunit interaction, and is more sensitive to inhibition by ATP. The simplest explanation of these results is that Mg^{2+} and Mn^{2+} stabilize two structurally distinct forms of the malic enzyme which vary in catalytic and regulatory properties. These results are strikingly similar to the results obtained with the isocitrate dehydrogenase system from *Neurospora crassa*, including the complex subunit interaction observed in the presence of Mg^{2+} (Barratt & Cook, 1978). The similar effects of Mg^{2+} and Mn^{2+} on two seemingly unrelated enzymes indicate that metal cofactors must be considered as important regulatory entities. Since *E. coli* is known to have specific transport systems for both Mg^{2+} and Mn^{2+} and can accumulate both cations even when grown on minimal media containing apparently no added Mn^{2+} (Silver, 1977; Silver & Jasper, 1977), control of the Mg^{2+}/Mn^{2+} ratio in the cell may turn out to be yet another level of control of cellular metabolism.

References

Apps, D. K. (1973) *Biochim. Biophys. Acta 320*, 379.

Barratt, D. G., & Cook, R. A. (1978) *Biochemistry 17*, 1561.

Coleman, R. F. (1972) *Anal. Biochem. 46*, 358.

Cook, R. A., & Koshland, D. E., Jr. (1970) *Biochemistry 9*, 3337.

Cornish-Bowden, A., & Koshland, D. E., Jr. (1975) *J. Mol. Biol. 95*, 201.

Davis, B. J. (1964) *Ann. N.Y. Acad. Sci. 121*, 404.

Deuel, T. F., & Stadtman, E. R. (1970) *J. Biol. Chem. 245*, 5206.

Gabrielli, F., & Baldi, S. (1973) *Experientia 29*, 1342.

Gentner, N., & Preiss, J. (1968) *J. Biol. Chem. 243*, 5882.

Hsu, R. Y., & Lardy, H. A. (1967) *J. Biol. Chem. 242*, 527.

Hsu, R. Y., Mildvan, A. S., Chang, G. G., & Fung, C. H. (1976) *J. Biol. Chem. 251*, 6574.

Koshland, D. E., Jr., Nemethy, G., & Filmer, D. (1966) *J. Mol. Biol. 12*, 88.

Matagne, R. F., & Schlosser, J.-P. (1977) *Biochem. J. 167*, 71.

Monod, J., Wyman, J., & Changeux, J. P. (1965) *J. Mol. Biol. 12*, 88.

Murai, T., Tokushige, M., Nagai, J., & Katsuki, H. (1972) *J. Biochem. (Tokyo) 71*, 1015.

O'Sullivan, W. J. (1969) in *Data for Biochemical Research, 2nd Ed.*, pp 423–434, Oxford University Press, London.

O'Sullivan, W. J., & Perrin, D. D. (1964) *Biochemistry 3*, 18.

Perrin, D. D., & Sayce, I. G. (1967) *Talanta 14*, 833.

Rose, I. (1968) *Proc. Natl. Acad. Sci. U.S.A. 61*, 1079.

Sanwal, B. D. (1970a) *Bacteriol. Rev. 34*, 20.

Sanwal, B. D. (1970b) *J. Biol. Chem. 245*, 1212.

Segal, A., & Stadtman, E. R. (1972a) *Arch. Biochem. Biophys. 152*, 356.

Segel, A., & Stadtman, E. R. (1972b) *Arch. Biochem. Biophys. 152*, 367.

Silver, S. (1977) in *Microorganisms and Minerals* (Weinberg, E. D., Ed.) p 49, Marcel Dekker, New York.

Silver, S., & Jasper, P. (1977) in *Microorganisms and Minerals* (Weinberg, E. D., Ed.) p 105, Marcel Dekker, New York.

Takeo, K. (1969) *J. Biochem. (Tokyo) 66*, 379.

Takeo, K., Murai, T., Nagai, J., & Katsuki, H. (1967) *Biochem. Biophys. Res. Commun. 29*, 717.

Weber, K., & Osborn, M. (1969) *J. Mol. Biol. 244*, 4406.

Wimhurst, J. M., & Manchester, K. L. (1970) *FEBS Lett. 10*, 33.

Yamaguchi, M., Tokushige, M., & Katsuki, H. (1973) *J. Biochem. (Tokyo) 73*, 169.

Yamaguchi, M., Tokushige, M., Takeo, K., & Katsuki, H. (1974) *J. Biochem. (Tokyo) 76*, 1259.

Zwaan, J. (1967) *Anal. Biochem. 21*, 155.